Film Cooling and Hub Disk Leakage Flow Experiments in a Fully Rotating HP Turbine Stage

M. PAU, A. DE LA LOMA, G. PANIAGUA AND D. DELHAYE
Turbomachinery and Propulsion Department
Von Karman Institute for Fluid Dynamics
Chaussée de Waterloo 72, B1640 – Sint Genesius Rode
BELGIUM

Abstract: - This paper describes the experimental methodology, test conditions, and flow physics concerning platform purge flow and film cooling experiments on a fully rotating HP transonic turbine stage under engine representative conditions. A complex secondary air system has been designed in order to feed the cooled turbine. The rotor blade has been heavily instrumented at the platform, 7% and 15% of the blade height with fast response pressure sensors and double-layer thin film gauges, allowing a complete aero-thermal characterization of the flow field. The hub disk leakage and platform cooling blowing ratios have been varied independently in order to assess their impact individually. Furthermore, tests have been performed at two different rotational speeds. The hub disk leakage flow has a strong impact on the flow field, changing the degree of reaction and the stage velocity triangles. The stator-rotor interaction is particularly affected by the stator rim cavity flow both in terms of heat transfer and pressure fluctuations.

Key-Words: - Gas turbine, leakage flows, film cooling.

1. Introduction

An increase of the specific work and cycle efficiency of gas turbines can be achieved through higher turbine inlet temperatures. Preserving an adequate life at these high temperatures requires efficient cooling methods. In high pressure turbine stages cold flow is also ejected from the cavity that exists between the stator rim and the rotor disk, in order to avoid hot gas injection into the wheel space cavity. The cold cavity flow is mostly entrained into the rotor hub vortex, Paniagua et al.[1], leaving the platform directly exposed to the hot gas, hence some portions of the rotor platform are unprotected, resulting in high thermal and mechanical stress buildup at the hub platform. Active platform cooling on those regions allows appropriate thermal isolation at the blade root, which may lead to platform cracking. Furthermore, the hub trailing edge region is then protected by film cooling ejection from the rear part of the platform.

Experimental investigations available in the open literature on film cooling and heat transfer on rotating turbine blades and their components are scarce, primarily due to the difficulties in instrumenting rotating parts. Dring et al. [2] investigated film cooling performance in a low speed rotating facility. A film cooling hole was located on both the pressure and suction sides. Their results show that the film coolant had only a small radial displacement, similar to flat plate results, on the suction side. On the pressure side, the film coolant trace had a large radial displacement toward the blade tip. Effectiveness distributions on the blade span for a rotating turbine blade were also provided by Takeishi et al. [3] and Abhari and Epstein [4] using gas chromatography and thin film heat flux gages respectively. Blair [5] studied the heat transfer on the pressure and suction sides as well as on the hub platform surface for a rotating turbine model. Enhanced heat transfer was observed on the platform due to the secondary flow effects. Recently, Ahn et al. [6] investigated film cooling effectiveness on the leading edge of a rotating blade using pressure sensitive paint (PSP) at design and off-design conditions. The off-design condition altered significantly the film coolant traces on the leading edge.

Platform film cooling and hub disk leakage investigations have been predominantly performed using cascade vanes. One of the earliest studies on platform film cooling was performed by Blair [7] using an upstream slot in a large scale turbine vane passage. Harasgama and Burton [8] conducted heat transfer and aerodynamic measurements in an annular cascade fitted with vanes under representative engine flow conditions. Their results show that film cooling reduced the Nusselt numbers near the suction side by about 50% suggesting that the coolant was convected towards the suction side by the passage secondary flows. Friedrichs et al. [9]

detailed the aerodynamic aspects of platform film cooling and the effectiveness distributions using the ammonia and diazo technique. The tests were performed in a large scale low-speed turbine cascade fitted with four rows of film cooling holes at 4 axial stations on the platform. The presence of secondary flows was found to erode the coolant film near the surface. The film cooling traces were observed to be pushed towards the suction side especially near the leading edge of the blade. It was also concluded that platform film cooling increase aerodynamic losses due to the mixing process.

Film cooling effectiveness distributions were measured by Zhang and Jaiswal [10] in a NGV using the pressure sensitive paint (PSP). High coolant-to-mainstream mass flow ratios were required to attain uniform effectiveness distribution. Kost and Nicklas [11] and Nicklas [12] performed aerodynamic and thermodynamic measurements in a film cooled linear transonic turbine cascade, with coolant injection through an upstream slot and at the cascade entrance. They found that slot injection dramatically strengthened the horseshoe vortex due to proximity of the slot to the leading edge.

Film cooling on the rotor platform under rotating conditions is still an uninvestigated phenomenon in the open literature.The current investigation was performed in a multipurpose turbine research facility with a new turbine to accommodate film cooling between the stator-rotor circumferential gap. Insightful information on the effects of blowing ratio, rotational speed and hub disk leakage is provided. The present research will furnish valuable data to calibrate advanced CFD tools, and advance our knowledge on the complex flow interactions in a cooled HP transonic turbine.

2. Nomenclature

C Chord [m]
HBL Hub disk leakage
M Mach number
P Pressure [bar]
Re Reynolds number $\rho \cdot V \cdot C / \mu$
S Curvilinear abscissa [m]
T Temperature [K]
t Time [s]
x Axial distance [m]

Subscripts

0 Total conditions
1 Stator inlet
2 Stator outlet, rotor inlet
3 Rotor outlet
r Relative conditions
ax axial
h hub
is isentropic

3. Experimental Apparatus

3.1 Turbine test rig

The measurements have been performed in the compression tube turbine test rig CT3 at the von Karman Institute. The heat transfer process of a real engine is reproduced in a short duration turbine test rig by a sudden release of hot gas over a cold turbine. The operation cycle of the rig is fully described by Dénos and Paniagua [13]. The turbine stage is composed of 43 cylindrical vanes and 64 cooled twisted blades.

The tip clearance is a parameter which strongly influences the turbine efficiency. Measurements have been done at design and off-design rotational speeds, at three different locations.

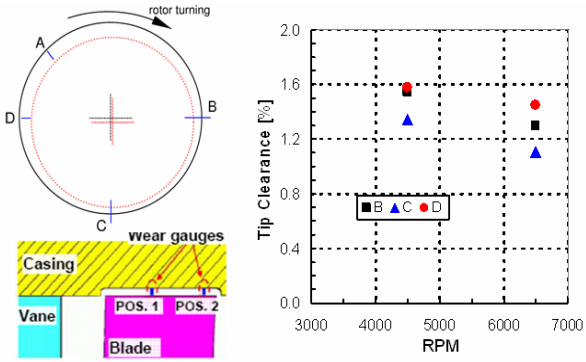

Figure 1: Wear gauges locations and changes of tip clearance with the rotational speed

At each peripheral location shown in Figure 1, two wear gauges are located at 45% and 80% of the blade axial chord. Figure 2 shows the tip clearance measured at position 1, as a percentage of the blade height. At 6500 RPM the mean level of tip clearance is 1.24%. A comparison between some relevant main stream features in the test rig and the actual engine configuration is illustrated in Table 1.

Main stream	Engine	Rig
Reynolds	10^6	10^6
T_{01} [K]	1800	440
T_{wall} [K]	1200	310
T_{wall} / T_{01}	0.67	0.67
P_{01} [bar]	20	1.62
P_{01}/P_{S3}	3	3
Massflow [kg/s]	50	10.84

Table 1: Engine-rig stage comparison

The gas to wall temperature ratio is respected in the experiments, as well as pressure

ratios and Mach and Reynolds number levels. Table 2 compares cooled rotor platform data in the engine and the rig. While the main stream to coolant pressure ratios encountered in actual film cooling schemes are easily matched, generally the target temperature ratio is more difficult to accomplish experimentally since very low coolant temperatures are required.

Platform	Engine	Rig
Ts main stream [K]	1398	330
Ps main stream [bar]	6.42	0.52
Mach main stream	0.85	0.85
P_{0r} coolant [bar]	7.8	Free
T_{0r} coolant [bar]	700	290 - 285
Pratio cooling holes	1.22	Free

Table 2: Engine-rig platform cooling comparison

3.2 Instrumentation

Capturing properly the aero-thermal impact of film cooling and inter-stage purge flow ejection in such an environment requires a significant effort in terms of instrumentation. Global quantities have been measured at three different locations along the turbine axis as depicted in Figure 2. Radial traverses of pressure and temperature have been performed upstream (plane 1) and downstream (plane 3) of the turbine stage using Kiel probes, static pressure taps and miniaturized type K thermocouples.

The static pressure at the vane exit (plane 2) ($0.035xC_{ax}$) is measured at 10 locations along the hub endwall, covering one stator pitch. The rotor-stator annular gap is instrumented on the stator rim with 10 pressure tappings distributed over one vane pitch. Both pneumatic taps and sub-surface mounted fast response transducers have been used.

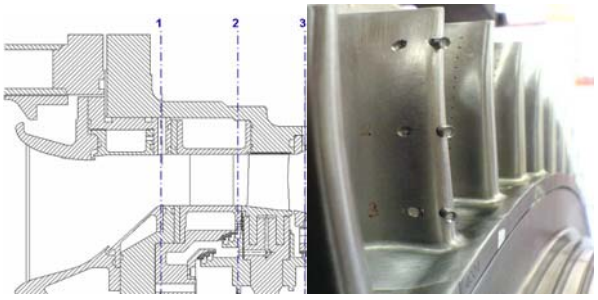

Figure 2: left - Meridional plane, right - LE Relative total pressure probes (15%, 50% and 85%)

Thin film gauge resistors mounted on an insulating substrate (Upilex) around the airfoil measure the heat transfer rates to turbine blades (Schultz and Jones, 1973). On the cooled rotor platform, due to the strong temperature gradients inside the metal, a second boundary condition is necessary to retrieve the heat flux, thus foil thermocouples have been placed underneath the gauges.

The rotor blade static pressure has been measured at 15% of the blade height and platform surface with high frequency response pressure sensors. The stagnation pressure at the rotor leading edge (15%, 50% and 85%) has been obtained with recessed Pitot probes as depicted in Figure 2. Since the rotor incidence angle changes at high frequency, the shield placed around the sensors allows retrieving accurately the stagnation pressure in the relative frame. The fast response instrumentation mounted on the rotor blades should ensure a frequency bandwith above 30 kHz to resolve the large vane passing pulsations (at 4.7 kHz) and its harmonics.

3.3 Cooling system

Significant changes to the previous experimental apparatus were implemented to meet the experimental objectives. In particular two heat exchangers and a pre-swirler were added to the existing hardware.

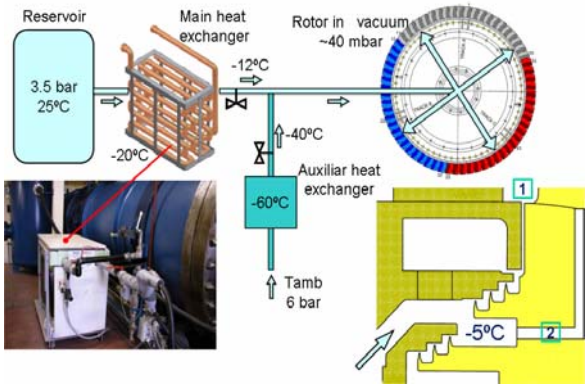

Figure 3: Turbine platform cooling scheme

Figure 3 shows an schematic of the coolant supply system. Well in advance performing a blow-down test, all the coolant path from the reservoir to the rotor is cooled down by means of a secondary heat exchanger operating at -60°C (Carbo-ice and Methanol). Once the temperature is satisfactory, the main reservoir is vented through a major heat exchanger (-20°C) allowing the required massflow rates. Before entering the rotor disk, the coolant air passes through a pre-swirler with an exit angle of 80°C (Figure 4). By swirling the flow at the rotor inlet, the total relative coolant temperature is kept low, up to 10 degrees lower with respect to the axial injection.

The coolant air finally reaches the rotor disk

cavity, where part of it is injected into the rotor (location 2), feeding the platform cooling holes, and the rest leaks through the labyrinth seals producing the hub disk leakage flow (location 1).

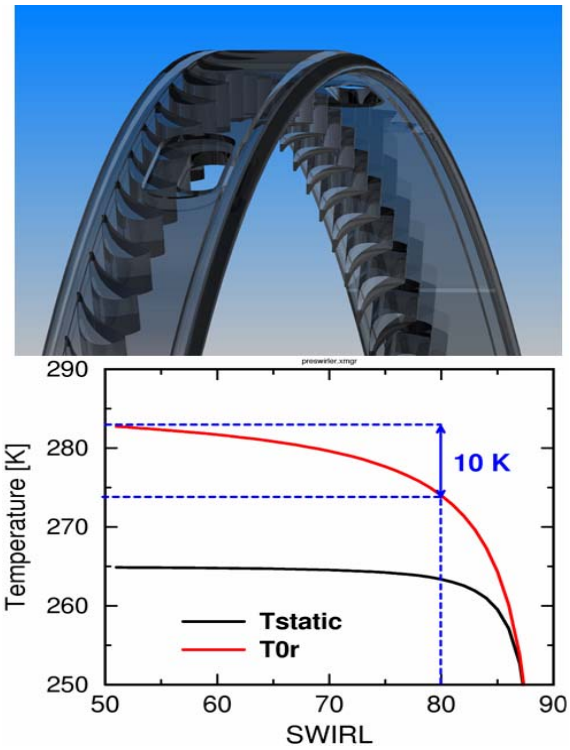

Figure 4: Pre-swirler 3D view and operating point at design conditions

Since both the platform film cooling and HDL flow come from the same cavity Figure 3, both blowing ratios are coupled and can not be varied independently. Along with airfoil surface heat transfer and pressure measurements, the data from inside the coolant path and plenums has been also investigated.

4. Experimental Results

4.1 Platform cooling design

The film cooling scheme on the platform is shown in Figure 5. The design comprises 5 cylindrical holes inclined at 30 deg. The location of the cooling holes on the platform was determined by considering: the direction of the streamlines over the platform; a similar static pressure field on the platform; hole spacing allowing instrumentation and preserving the mechanical integrity.

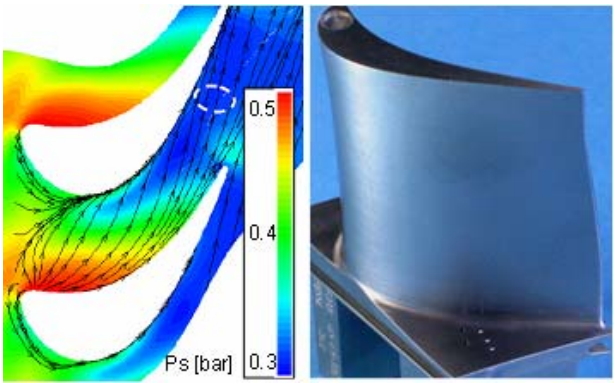

Figure 5: Computed streamlines and view of the platform cooling holes

4.2 Test Conditions and methodology

Four different operating conditions have been designed in order to assess independently the purge flow impact and the platform film cooling. The baseline experiment, without coolant injection and at nominal speed (6500rpm), is consequently compared to the other 3. The effect of the rotational speed on the platform cooling has been analyzed performing off design tests (4500 RPM).

Condition	m_{elbow} [%]	m_{blade} [%]	m_{HDL} [%]	RPM
Baseline	0.00	0.020	-1.00	6500
Blade Cooling	1.52	0.043	0.28	6500
Off Design	1.51	0.038	0.15	4500
HD Leakage	1.99	0.040	0.76	6500

Table 3: Measured coolant flow rates at different operating condition

Table 3 illustrates the measured coolant massflow rates expressed as a percentage of the main stream massflow for the different operating conditions. The massflow fed into the rotor blade is computed based on the total relative pressure and temperature measured in rotation inside the coolant channel (location 2 in Figure 3) and the static pressure field in the platform at the location of the film cooling holes.

The mass flow ingested or ejected in the hub cavity is computed as the difference between the total coolant flow rate supplied by the system and the mass flow leaking towards the inner chamber (location 3) through the lower labyrinth seal. The supply massflow is controlled with choked orifices. The flow rate entering the inner chamber is computed based on the known volume of the chamber and the pressure and temperature evolution during the test, as shown in Figure 6.

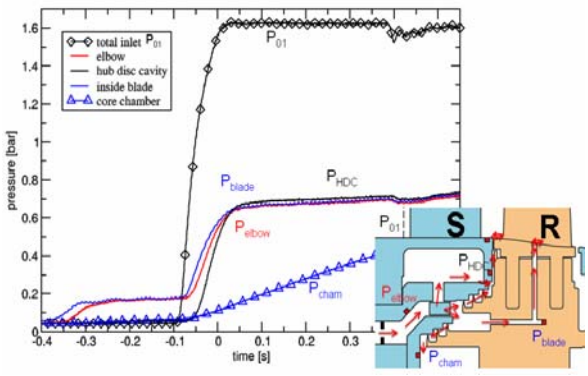

Figure 6: Pressure evolution during the test

Figure 6 shows pressure traces at different locations in the coolant path together with the evolution of the stage total inlet pressure P_{01} during the actual testing time (~0.4 s). The coolant injection starts 0.35 seconds before the actual blow down, allowing thus the full development of the coolant flow. Once the desired blowing ratios are steady, the high pressure and temperature main stream gas is vented through the stage producing the sudden increase in P_{01}. The pressure rise in the main stream channel pressurizes all the inner cavities, remaining constant afterwards during the blow down time.

At the baseline condition, without any coolant ejection, the mass flow into the inner cavity is ~1 % of the mainstream mass flow, consequently, hot gas ingress occurs (at a rate of 1 %) in the absence of cavity coolant flow ejection, driven by the low pressure inside the chamber.

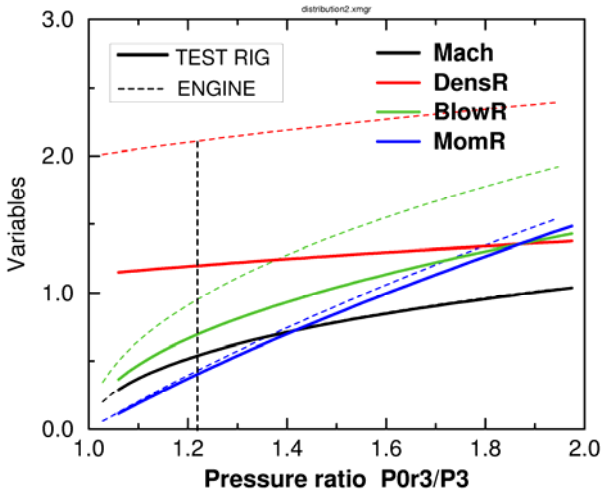

Figure 7: Film cooling parameters, comparison rig-engine

Figure 7 shows the evolution of the different film cooling parameters as a function of the pressure ratio across the holes for the rig configuration and engine conditions. The blowing ratio can be easily varied in order to match the engine configuration. However the rig density ratio is far from the actual density ratio encountered in actual film cooling practice. To match the density ratio expensive cryogenic techniques are required, an alternative solution is to utilize a denser gas.

4.3 Stator outlet flow field

The static pressure distribution in the hub disc cavity and at the hub downstream of the stator is shown in Figure 8 for three conditions, without coolant ejection, with hub disk leakage and with blade platform cooling. While the static pressure stays constant along the pitch inside the cavity, it varies up to 19 % at the hub endwall due to the shock system created by the stator.

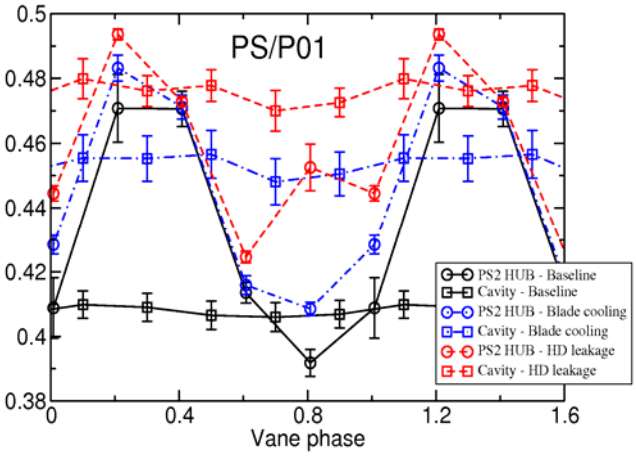

Figure 8: Pitch wise variation of the static pressure at the stator – rotor interface.

The comparison of the different conditions reveals that increasing the ejected mass flow leads to an increase of the static pressure in both locations. For each condition, the coolant ejection and ingestion zones are clearly identified analyzing the different curve levels. A higher pressure in the cavity than in the mainstream flow leads to ejection of air out of the cavity while the opposite situation leads to ingestion. In the baseline condition, the mainstream gas enters the cavity over more than 60 % of the pitch at a net rate of 1 %. The ratio is reversed in the "blade cooling" condition: air enters the cavity over less than 40 % of the pitch, resulting in a net coolant rate ejected to the mainstream of 0.26 %. Finally, in the "hub disk leakage condition", the net coolant rate is of 0.76 % and air is ejected nearly over the whole span except close to the left running trailing edge shock which causes a compression of the mainstream gas.

Table 4 shows the measured average values of pressure ratio, Mach number downstream of the

stator, reaction degree and power. When the ejection rate is increased, a larger blockage effect is detected, which leads to a lower Mach number downstream of the stator and a higher pressure ratio across the vane hub.

Condition	P_{s2h}/P_{01}	$M_{2is,h}$	R_h	P_{01}/P_{s3}	Power [kW]
Baseline	0.433	1.16	0.236	3.13	991.579
Blade Cooling	0.442	1.15	0.251	3.12	990.650
Off Design	0.417	1.19	0.209	3.14	837.221
HD Leakage	0.459	1.12	0.278	3.10	974.914

Table 4: Pressure ratio, Mach number, degree of reaction and measured Power

As a consequence, the rotor inlet Mach number decreases locally, modifying the incidence in the relative frame and increasing the reaction degree at the hub. The power decreases with the increasing of the injected coolant flow rate.

The effect of hub disc leakage on the total relative pressure at the leading edge of the rotor blades is illustrated in Figure 9. The effect of the ejected air on the channel blockage is perceived in all three measuring locations, at 15 %, 50 %, and 85 % of the span.

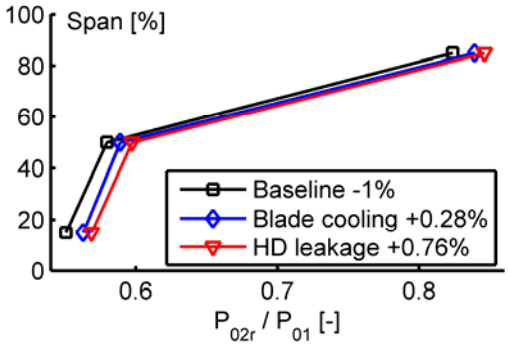

Figure 9: Static pressure distribution at the rotor leading edge.

Compared to the baseline condition, for which there is negative blockage due to the ingestion, the pressures are respectively 1.9 % and 3.0 % higher on average for the "blade cooling" and "hub disc leakage" conditions. The blockage effect is highest at the hub where the pressures are respectively 2.2 % and 3.3 % higher than the baseline.

4.4 Stage outlet flow field

The radial variation of the total pressure and temperature is reported in Figure 10. The measurements were performed in a fixed pitch-wise location, aligned with the leading edge of the vane, along the radius. The conditions which are plotted correspond to the baseline condition (0), to the off-design condition (3), and to the hub disk leakage and film cooling ejection (4).

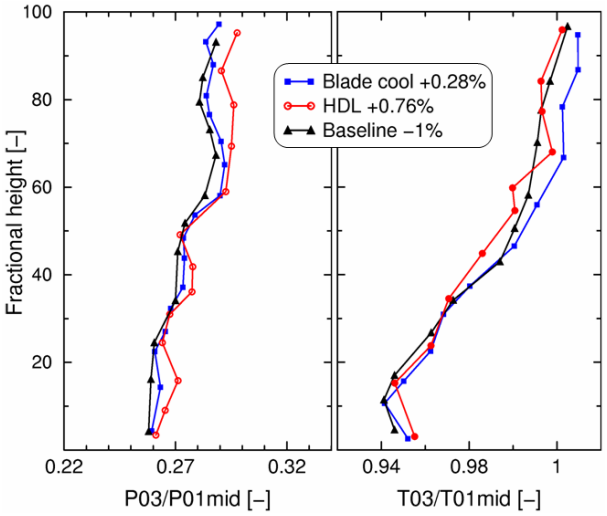

Figure 10: Span-wise total temperature and pressure distribution at the stage outlet

The total pressure shows an overall increase of P_{03}/P_{01} due to the cavity flow injection. For the off-design condition the average total pressure is higher along the whole span. The drop in temperature due to the mixing of the coolant and the free stream hot gas close to the hub cannot be clearly identified, probably because it is within the experimental repeatability.

5. Conclusions

Hub disk leakage and hub rotor platform film cooling experiments have been carried out in a fully rotating HP transonic turbine stage under engine representative conditions. Several test conditions have been tested in order to analyze independently the effects of the rotor platform cooling, the hub disk leakage, and the rotational speed.

The turbine test rig has been modified in order to provide the required coolant flow rates and temperatures. Two heat exchangers have been used to cool down the flow injected in the turbine. Hub disk leakage coolant flow injection from the stator-rotor rim cavity contributes to a blockage effect which results in a lower transonic loading of the turbine, with reduced Mach numbers at the stator outlet and with increased pressure ratio across the vane row. Larger coolant flow rates correspond to a decrease of incidence in the relative rotor frame,

thus increasing the degree of reaction at the hub. The pitch-wise variation of the stator-rotor interface cavity flowfield, the coolant mass flow exchange between the cavity and the main channel was found to be mainly dictated by the shock structure interactions downstream of the stator trailing edge.

6. Acknowledgments

The authors would like to acknowledge Bertrand Haguenauer and Tolga Yasa for their assistance in the testing. The authors would also like to acknowledge the financial support of the European Commission and Industrial Partners involved in TATEF2 "Turbine Aero-Thermal External Flows 2".

7. References

[1] Paniagua, G., Denos, R., Almeida, S., 2004, "Effect of the Hub Endwall Cavity Flow on the Flow Field of a Transonic High-Pressure turbine," ASME J. of Turbomachinery, **126**, pp. 578-586.

[2] Dring, R. P., Blair, M. F., and Hoslyn, H. D., 1980, "An Experimental Investigation of Film Cooling on a Turbine RotorBlade," ASME J. of Engineering for Power, **102**, pp. 81-87.

[3] Takeishi, M., Aoki, S., Sato, T., and Tsukagoshi, K., 1992, "Film Cooling on a Gas Turbine Rotor Blade," ASME J. of Turbomachinery, **114**, pp. 828-834.

[4] Abhari, R.S., and Epstein, A.H., 1994, "An Experimental Study of Film Cooling in a Rotating Transonic Turbine," ASME J. of Turbomachinery, **116**, pp. 63-70.

[5] Blair, M.F., 1994, "An Experimental Study of Heat Transfer in a Large-Scale Turbine Rotor Passage," ASME J. of Turbomachinery, **116**, pp. 1-13.

[6] Ahn, J., Schobeiri, M.T., Han, J.C., and Moon, H.K., 2004, "Film Cooling Effectiveness on the Leading Edge of a Rotatine Turbine Blade," IMECE 2004-59852.

[7] Blair, M.F., 1974, "An Experimental Study of Heat Transfer and Film Cooling on Large-Scale Turbine Endwalls," ASME J. of Heat Transfer, pp. 524-529.

[8] Harasgama, S.P., and Burton, C.D., 1992, "Film Cooling Research on the Endwall of a Turbine Nozzle Guide Vane in a Short Duration Annular Cascade: Part 1 – Experimental Technique and Results," ASME J. of Turbomachinery, **114**, pp.734 740.

[9] Friedrichs, S., Hodson, H.P., Dawes, W.N., 1996, "Distribution of Film-Cooling Effectiveness on a Turbine Endwall Measured Using Ammonia and Diazo Technique," ASME J. of Turbomachinery, **118**, pp.613-621.

[10] Zhang, L.J., and Jaiswal, R.S., 2001, "Turbine Nozzle Endwall Film Cooling Study Using Pressure Sensitive Paint," ASME J. of Turbomachinery, **123**, pp.730-738.

[11] Kost, F., and Nicklas, M., 2001, "Film-Cooled Turbine Endwall in a Transonic Flow Field: Part 1 – Aerodynamic Measurements," ASME J. of Turbomachinery, **123**, pp.709-719.

[12] Nicklas, M., 2001, "Film-Cooled Turbine Endwall in a Transonic Flow Field: Part 2 – Heat Transfer and Film-Cooling Effectiveness," ASME J. of Turbomachinery, **123**, pp.720-728.

[13] Dénos, R. and Paniagua, G., 2005-b: "Rotor/Stator interaction in Transonic HP Turbines". VKI Lecture Series on "Effects of Aerodynamic Unsteadiness in Axial Turbomachines". VKI LS 2005-03. ISBN: 2-930389-59-1. Sint Genesius Rode.